Title: Leptin-Associated Sex Difference in TMJ OA Induced by Metabolic Endotoxemia

Authors: Shipin Zhang[1*], Siyi Chen[1], Marina Fonti[1], David Fercher[1]

Affiliations: [1]Department of Health Sciences and Technology, Institute for Biomechanics, Tissue Engineering and Biofabrication Group, ETH Zürich, Switzerland

[*] Correspondance : shipin.zhang@hest.ethz.ch

ORCIDs:

Shipin Zhang (https://orcid.org/0000-0001-8421-7108)

Siyi Chen (https://orcid.org/0009-0008-6462-4441)

Marina Fonti (https://orcid.org/0000-0002-2415-8019)

David Fercher (https://orcid.org/0009-0000-8934-9441)

Keywords: Temporomandibular disorders (TMD), Endotoxins, Inflammation, Systemic health/disease, Obesity, Receptors

Total word count for abstract: 300

Total word count from abstract to acknowledgement: 3643

Total number of figures: 4

Total number of tables: 0

Number of references: 30

Abstract

Temporomandibular joint (TMJ) osteoarthritis (OA) is a degenerative disease affecting cartilage, bone and synovium. Factors such as age, sex and obesity are associated with TMJ OA, however, the underling mechanisms, particularly the contribution of obesity, remain poorly understood. Unlike weight-bearing joints, TMJ pathology cannot be fully attributed to aberrant mechanical loading, suggesting a potential involvement of systemic metabolic factor. Evidence have linked metabolic endotoxemia, characterized by subclinical elevation of plasma lipopolysaccharide (LPS) level to low-grade systemic inflammation, adipose tissue dysfunction and adipokine dysregulation. Among adipokines, circulating leptin has been associated with OA progression, but its role in the onset and progression of TMJ OA, especially in a sex-specific context, is under studied.

In this study, we examined whether chronic systemic LPS could induce adipose tissue abnormalities and leptin signalling dysregulation, contributing to TMJ OA. The metabolic endotoxemia was induced in 6-month-old female and male Wistar rats via systemic LPS delivery for 6 weeks using subcutaneously implanted osmotic pumps. At the end of the study, the peripheral blood, subcutaneous and visceral white adipose tissue, and TMJs were harvested for various analyses.

We showed that LPS-treated female rats showed elevated circulating LPS and adipocyte hypertrophy in white adipose tissue. This was accompanied by increased plasma leptin concentrations. These changes were not observed in male rats. Histological evaluation of TMJ revealed pronounced osteoarthritic changes in TMJ, characterized by cartilage matrix loss, subchondral bone resorption, and synovial inflammation, in female but not male rats. Immunofluorescence staining discovered differences in the distribution and expression of nitric oxide and leptin receptor in cartilage between sexes. Correlation analysis suggested the involvement of leptin in TMJ OA.

In conclusion, we demonstrated that systemic LPS promoted sex-specific TMJ OA through leptin-mediated inflammation, suggesting a potential systemic-to-local link between endotoxemia, adipose dysfunction, and TMJ OA pathogenesis in female.

Introduction

The temporomandibular joint (TMJ) is a low/non-weight-bearing synovial joint in the oral maxillofacial area. TMJ osteoarthritis (OA) is a degenerative disease characterized by cartilage surface fibrillation, glycosaminoglycan (GAG) loss, bone resorption and synovitis. Proposed risk factors for TMJ OA include age, sex, obesity, and craniofacial abnormalities (Wang et al. 2015). Among various risk factors, age and sex are widely accepted important contributors. Middle-aged women experience a significantly higher incidence of TMJ OA than men (Alzahrani et al. 2020; Yadav et al. 2018).

Recent research has found obese individuals are more likely to develop TMD symptoms than their lean counterparts (Minervini et al. 2023). The mechanism linking obesity and TMJ OA cannot be fully explained by excessive biomechanical loading, as TMJ is not a weight-bearing joint. This suggests the potential contribution of systemic metabolic factors in the onset and development of TMJ OA. One possible mechanism is adipose-driving cytokine signalling. Leptin, an adipokine secreted by white adipose tissue (WAT), has been implicated in OA pathogenesis (Ait Eldjoudi et al. 2022; Du et al. 2020), where elevated leptin levels correlate with systemic inflammation, cartilage damage and synovial inflammation(Lago et al. 2008). It's been hypothesized that higher prevalence of OA in women could be attributed to higher leptin concentration in females (Teichtahl et al. 2005). However, the exact stimuli triggering the dysregulation of leptin and its sex-specific role in TMJ OA remain unexplored.

Metabolic endotoxemia, a state of chronically elevated circulating endotoxin or lipopolysaccharide (LPS) – may represent a key upstream stimulus. LPS is known to induce low-grade systemic inflammation, and has been shown to increase in both obese individuals (Pussinen et al. 2011; Trøseid et al. 2013) and high-fat-diet fed rodents (Amar et al. 2008; Cani et al. 2007; Collins et al. 2015). These findings suggest a possible link between endotoxemia and inflammatory reactions in adipose tissue, potentially disrupting adipokine balance and promoting joint degeneration.

Despite these associations, it remains unelucidated whether metabolic endotoxemia contributes to TMJ OA development through adipose tissue dysfunction and leptin signalling. Furthermore, the biological basis of sex differences in TMJ OA development is not fully understood.

The objective of this study is to evaluate the effects of chronic systemic LPS exposure on TMJ OA development. Specifically, we aim to identify the involvement of adipose tissue and adipokine signalling, with a focus on sex-specific responses. To achieve this goal, we systemically administrated LPS to female and male rats for six weeks. Ten weeks after the start of the LPS administration, we evaluated systemic inflammatory changes in blood plasma and adipose tissues, as well as osteoarthritic changes in TMJ cartilage, bone and synovium.

2. Method:

2.1 Animal experiment

The animal study was approved by the Veterinary Office of the Canton Zürich (License No. ZH158/2021) and conducted in accordance with ARRIVE guidelines. A total of Sixteen Wistar

rats (6 months old, Janvier Labs France) with a mean weight of male:365 g (372 – 471 g) and female: 298 g (262 – 330 g) were used in this study. The animals were randomised into two groups by block randomization method (Altman and Bland 1999) - LPS group (4 females and 4 males) and Saline group (4 females and 4 males). Osmotic minipumps (Alzet 2006, DURECT Corporation, USA) filled with 200µL of either 0.9% NaCl (B. Braun, Germany) or LPS from Escherichia coli (*E. coli*) O26:B6 (Sigma-Aldrich, USA) in 0.9% NaCl was implanted subcutaneously in the rats (Figure 1A). Metabolic endotoxemia was induce by continuous delivery of LPS solution at a rate of 18 µg/kg/day LPS for 42 days via the minipump (Figure 1B). Animals were housed in groups of 2 in individually ventilated cages in a standard laboratory animal environment (21± 3 °C and 12/12h light–dark cycle), received acidified tap water (pH 2.5-3.0) and standard laboratory rodent diet (KLIBA NAFAG, CH) in a specific opportunistic pathogen free facility. Ten weeks after the pump implantation, animals were euthanized by CO_2 overdose. Various samples were harvested for different analysis (Figure 1B).

2.2 Blood analysis

At the end of the study, 1 mL whole blood was collected post-mortem via cardiac puncture into a BD Vacutainer® EDTA Tubes (BD, USA). Plasma was prepared by centrifuging the whole blood for 10 min at 1500 g to remove cells and then at 2000 g to deplete platelets. Plasma was diluted 50 times with endotoxin-free water for LPS concentration analysis by LAL assay kit, or diluted 3 times for leptin quantification using an ELISA kit (Merck, USA). All assays were performed according to manufacturer's instructions.

2.3 Micro-computed tomography evaluation

After euthanasia, the heads were dissected and fixed at 4% (v/v) paraformaldehyde (PFA). High resolution micro-computed tomography (µCT) (µCT45, SCANCOMEDICAL) was performed to assess bone morphology. Samples were scanned coronally at 70kV, 57µA with a 4W spot size using a 0.5mm aluminium filter. A total of 1500 projections per 180° rotation with an integration time of 3096 ms were acquired and then reconstructed into a stacked of scans with a 10.4 µm-effective voxel size. A QC phantom (KP45, Diameter 34mm) (A09300, SCANCOMEDICAL) was used to calculate the bone mineral density reference standards. Volume of interest of the TMJ condyle was generated and export to a stack of TIFF images for 3-dimensional (3D) rendering in SCANCOMEDICAL applications. For bone parameter analysis, a stack of 200 coronal slides across the entire condyle were selected. The percentage of bone volume over total volume (BV/TV, %), trabecular thickness (Tb.Th, µm), trabecular separation (Tb. Sp, µm), trabecular number (Tb. N, 1/mm), and bone mineral density (BMD) were quantified using CTAn version 1.13 (Bruker microCT, Kontich, Belgium).

2.4 Histological analyses

After animal euthanasia, WAT were sampled from dorsolumbar subcutaneous adipose depot (SAT) and mesenteric visceral adipose depot (VAT), as previously described (Bagchi and MacDougald 2019). WATs were fixed in 4% PFA for 3 days before histological processing. Following µ-CT examination, the fixed heads were decalcified in aqueous 10% NH_4-EDTA solution for 3 weeks and trimmed to the TMJ region before processed for histology. Tissues were dehydrated on a Milestone Logos J device (Milestone, ITA) and embedded in paraffin wax as previously described (Weber et al. 2024). Serial sections were cut at 5 µm. WATs and

TMJs were stained with haematoxylin and eosin (H&E) for general morphology. TMJs were stained for Safranin-O/fast green (Saf-O) for GAG deposition and picrosirius red for fiber orientation (Asadikorayem et al. 2025). The stained sections were scanned using slide scanner Panonoramic 250 (3DHistech, Hungary) with 20x objective.

Histomorphometric analysis of adipocytes was performed on H&E images using QuPath v0 and ImageJ software (National Institutes of Health). The size of 2000 – 4000 adipocytes was measured, averaged and presented as the mean size of adipocyte for each sample.

The Saf-O-stained area in condylar cartilage was measured and normalized against the total area of cartilage layer to calculate the percentage (%) of Saf-O^+ area as previously described (Zhang et al. 2019). Mankin scoring (Mankin et al. 1971) was performed on Saf-O stained TMJs to evaluate the surface roughness, s-GAG deposition and structural integrity. Krenn's synovitis score (Krenn et al. 2006) was performed on H&E-stained slides to assess the inflammatory status of synovial membrane. Histopathological scoring of TMJ condylar cartilage and synovial membranes were performed by two blinded observers independently.

Sections stained with picrosirius red were imaged using Slideview TM VS200 (Evident/Olympus, Japan) with 0° rotation angle. The condylar cartilage was divided into two layers: top layer (T) consisting of superficial, proliferative and mature zones; and hypertrophic layer (H) consisting of hypertrophic zone for subsequent image analysis. The fiber orientation and energy evaluation was carried out using the OrientationJ plugin in ImageJ software (Rezakhaniha et al. 2012).

2.5 Immunofluorescence imaging

Immunofluorescent (IF) staining was performed to detect the expression of inducible nitric oxide synthase (iNOS) and leptin receptor (LEP-R) in TMJ condylar cartilage. Briefly, sections were deparaffinized, rehydrated and cooked in citrate buffer (pH6) at 60°C for 1 hour. After blocking for 1 hour with 5% (w/v) bovine serum albumin, the sections were incubated sequentially with anti-iNOS antibody (Abcam, ab15323, 1:100 dilution) and leptin receptor (Invitrogen, MA5-35247, 1:200) at 4°C overnight. Following each incubation, the sections were rinsed in PBS with 0.1% (v/v) Tween-20 and stained with Alexa Fluor 555 goat anti-rabbit IgG (1:500) or Alexa Fluor 647 goat anti-rabbit IgG (1:500) for 1 hour at ambient temperature. Cell nuclei were counterstained with 4′,6-diamidino-2-phenylindole (DAPI). The IF-stained slides were then imaged using Slideview TM VS200 (Evident/Olympus, Japan). DAPI-stained nuclei, iNOS positive (iNOS$^+$), LEP-R- positive cells (LEP-R$^+$), and iNOS/LEP-R double positive (Double$^+$) cells were counted in top and hypertrophic layer of condylar cartilage using ImageJ. The percentage of iNOS$^+$, LEP-R$^+$, and double$^+$ cells were calculated relative to the total number of DAPI-stained cells.

2.5 Statistics

SPSS version 29.0 (IBM, Chicago, IL, USA) was used for statistical analysis. Each animal is counted as one experiment unit for blood analysis, adipose size quantification, and weight change. Each joint is counted as one biological sample for quantification of Saf-O^+ area, histological scorings, fiber orientation analysis, μCT evaluation and IF quantification. Mann-Whitney U test was used to compare between two groups. All the analysis was done blindly.

All data were presented as median (95% CI), unless otherwise stated. Spearman correlation was used to evaluate the association between two variables, and the data presented as r (Spearman correlation coefficient), n (sample size), P (statistical significance level). Inter-class correlation coefficient (ICC) was calculated to assess the consistency of histopathological scores between the two independent observers. Statistical significance level was set as $P < 0.05$.

3. Results

3.1 Sex-specific effects of chronic systemic LPS exposure on adiposity and leptin production.

Plasma LPS concentration were comparable between healthy female (0.54 EU/ml, 95%CI: 0.46 – 0.64 EU/ml) and male rats (0.57 EU/ml, 95%CI: 0.28 – 1.06 EU/ml), indicating no sex difference in circulating endotoxin level under physiological condition. Continuous administration of LPS for 6 weeks significantly increased the plasma LPS concentration in female rats (1.08 EU/ml, 95%CI: 0.40 – 2.01 EU/ml, $P = 0.029$) compared to control females. On the contrary, the endotoxin level in LPS-treated male rats remained as low as that in healthy male controls (0.50 EU /ml, 95%CI: 0.48 – 0.54 EU/ml), and was significantly lower than that in female LPS group ($P = 0.029$) (Figure 1C).

The elevation of plasma LPS concentration in female led to adipocyte hypertrophic changes ($r = 0.762$, $n = 8$, $P = 0.028$). Relative to control group, adipocyte area increased by 24% in SAT (2081.50 μm^2, 95%CI: 1812.06 – 2321.94 μm^2, $P = 0.029$) and 23% in VAT (3462.00 μm^2, 95%CI: 3083.17 – 3748.83 μm^2, $P = 0.029$). In male rats, the adipocyte hypertrophic change was observed in SAT but not in VAT (Figure 1D, E).

Although the enlargement of adipocytes did not result in a significant weight gain (Figure 1F),the increase in adiposity in female rats was accompanied by an elevation in blood leptin concentration (15.58 ng/ml, 95%CI: 11.26 – 20.22 ng/ml) compared to healthy controls (9.76 ng/ml, 95%CI: 5.19 – 15.59 ng/ml, $P = 0.114$) (Figure 1G). Plasma leptin concentration showed moderate correlation with larger adipocyte sizes in both SAT ($r = 0.524$, $n = 8$, $P = 0.183$) and VAT ($r = 0.619$, $n = 8$, $P = 0.102$). In contrast, the leptin level in LPS-treated male rats did not differ from that in healthy control males and was not associated with the adipocyte size.

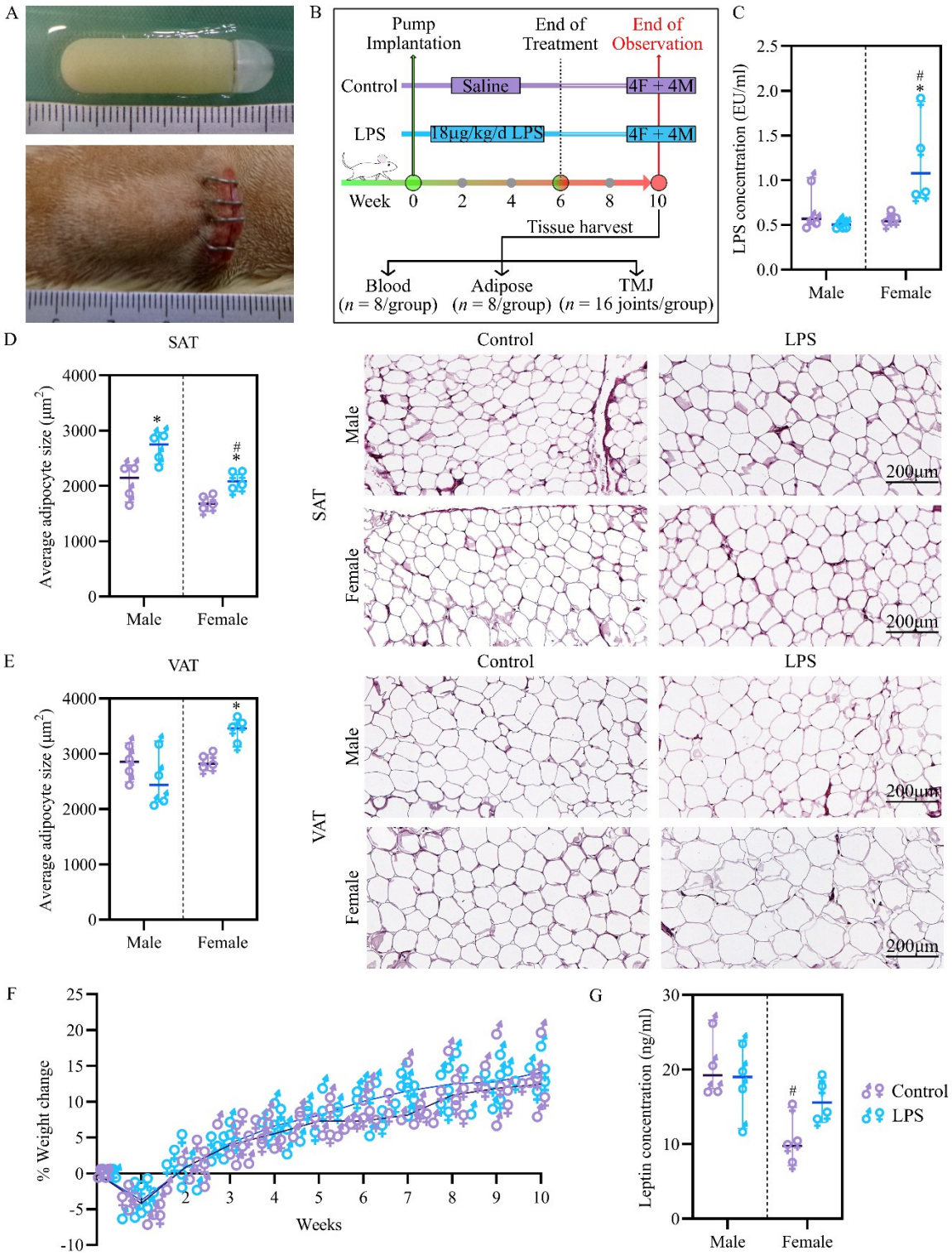

Figure 1. Chronic LPS exposure induces sex-specific changes in adipose tissue and leptin concentration. (A) Surgical pictures of the osmotic minipump implantation and (B) study timeline. (C) Plasma LPS concentration measured 10 weeks after pump implantation. The average area of adipocytes in (D) SAT and (E) VAT. (F) Longitudinal body weight change normalized to pre-surgery weight. (G) Plasma leptin concentration. Data are presented as median with 95% CI. N = 4 animals per group. * $P < 0.05$ compared to control group within same sex. # $P < 0.05$ compared male within the same treatment group.

3.2 Sex-specific TMJ osteoarthritic changes in cartilage, bone and synovial membrane

To assess cartilage degeneration, TMJs were first stained with Saf-O to visualize the general joint morphology and GAG content in cartilage matrix. Compared to controls, LPS-treated male rats showed mild GAG loss, predominately in the top layer. In contrast, LPS-treated female rats exhibited significant GAG loss throughout the entire cartilage (Figure 2A). Semi-quantitative analysis of GAG deposition confirmed this observation (Figure 2B). Female rats in LPS group had significantly lower percentage of Saf-O^+ area (36.6%, 95%CI: 25.81 – 45.03%) compared to control females (47.48%, 95%CI: 38.13 – 58.28%, $P = 0.05$) and LPS-treated males (56.37%, 95%CI: 36.95 – 71.39%, $P = 0.015$).

Consistently, LPS-treated females showed increased cartilage degeneration, featured by slight to moderate reduction in matrix staining, resulting a higher total Mankin score (4.50, 95%CI: 4.01 – 5.49) compared to control females (3.50, 95%CI: 3.12 – 4.38, $P = 0.038$) (Figure 2C, E). LPS-treated male rats also exhibited a higher Mankin score (4.75, 95%CI: 2.90 – 6.23) compared to control males (2.25, 95%CI: 1.39 – 3.73, $P = 0.038$), although the increase was likely due to surface irregularity rather than matrix loss (Figure 2C, D).

To further explore the cartilage structural changes, picrosirius enhanced polarized microscopy was performed to examine the organization of cartilage extracellular matrix (ECM). A pseudo-color map was generated to visualize ECM fibers orientation, with cyan color indicting predominantly horizontal alignment (Figure 2F). ECM derangement was clearly seen in LPS-treated male rats, where top-layer fibers were oriented primarily along the cartilage surface (7.00°, 95%CI: 4.03 – 11.76°), compared to control males is 15.49° (95%CI: 9.87 – 18.28°, $P = 0.028$) from the articular surface (Figure 2G). The matrix disorganization was less evident in female rats, where fiber orientation in both control and LPS-treated female rats was below 10°.

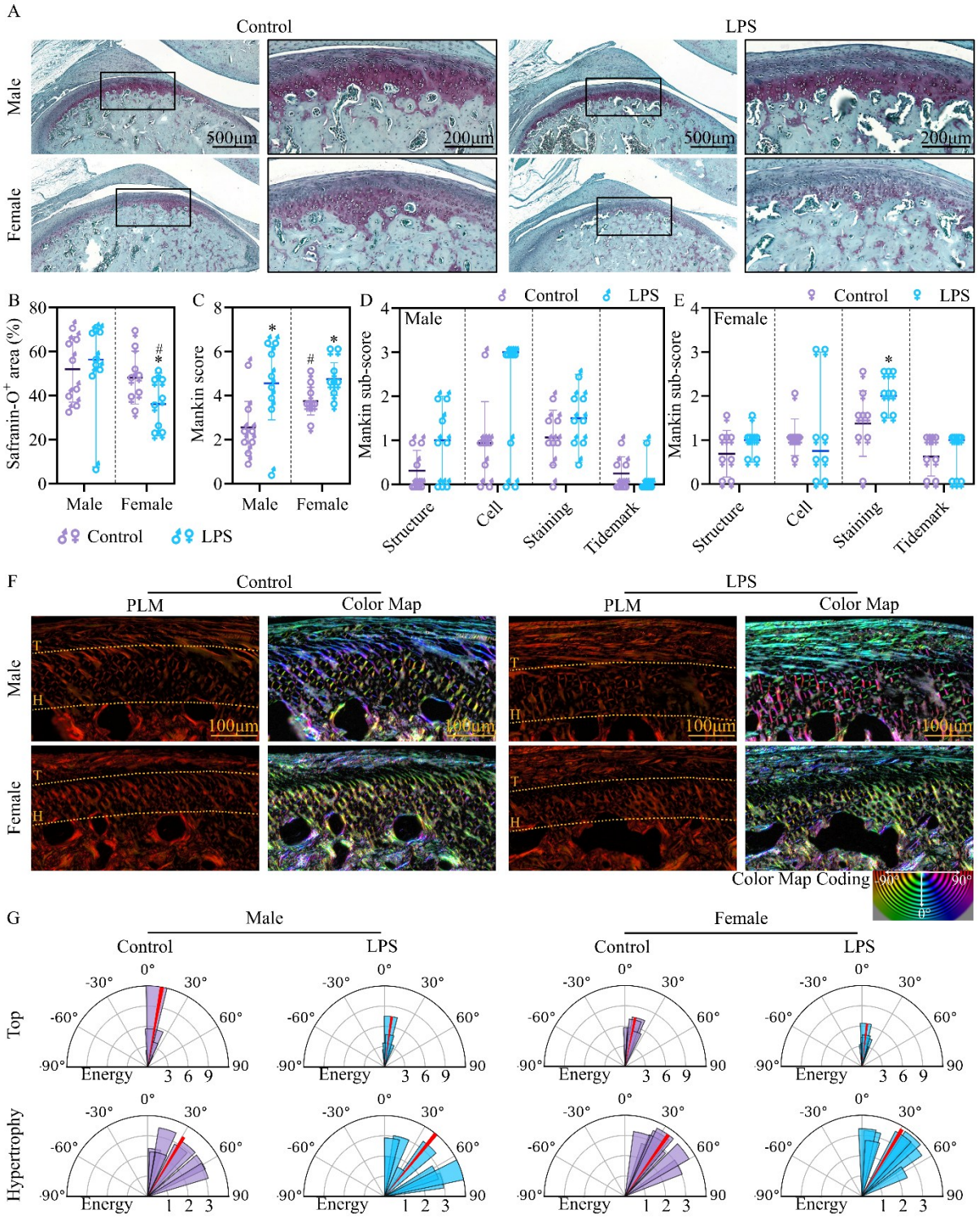

Figure 2. Histopathological evaluation of TMJ cartilage matrix deposition and ECM fiber organization in TMJ. (A) Representative images of TMJ stained with Saf-O. (B) Quantification of Saf-O^{+} area in condylar cartilage. (C) Total Mankin scoring and subcategory scores for (D) male and (E) female rats. (F) Picrosirius red-enhanced polarized microscopy was performed to assess ECM fiber organization, and pseudo-color mapping was used to visualize the fiber orientation. T: top layer and H: hypertrophic layer. (G) Rose plots illustrate the distribution of fiber orientation angles at top and hypertrophy layers. The red bar represents the population mean. N = 8 joints per group. Data are presented as median with 95% CI (except for the rose

plot). * $P < 0.05$ compared to control group within same sex. # $P < 0.05$ compared male within the same treatment group.

Changes in bone structural parameters were quantified in μCT (Figure 3A). Relative to males, female rats generally had lower percentage of BV/TV, attributing to higher number of thinner trabecular bone and bigger trabecular separation (Figure 3B). LPS exposure further reduced the Tb.N and increased Tb.Sp in female rats, leading to a significant reduction in BV/TV compared to control females ($P = 0.028$). Additionally, BMD in LPS-treated females was reduced by 10% compared to control females ($P = 0.01$). In contrast, chronic LPS exposure did not significant affect subchondral bone mass, architecture or mineral density in male rats (Figure 3B).

Finally, synovial inflammation was evaluated by Krenn's synovitis score (Figure 3C). Mild synovitis was observed only in female LPS group (Figure 3D), while no significant difference was noted in any of the subcategories in either sex (Figure 3E, F).

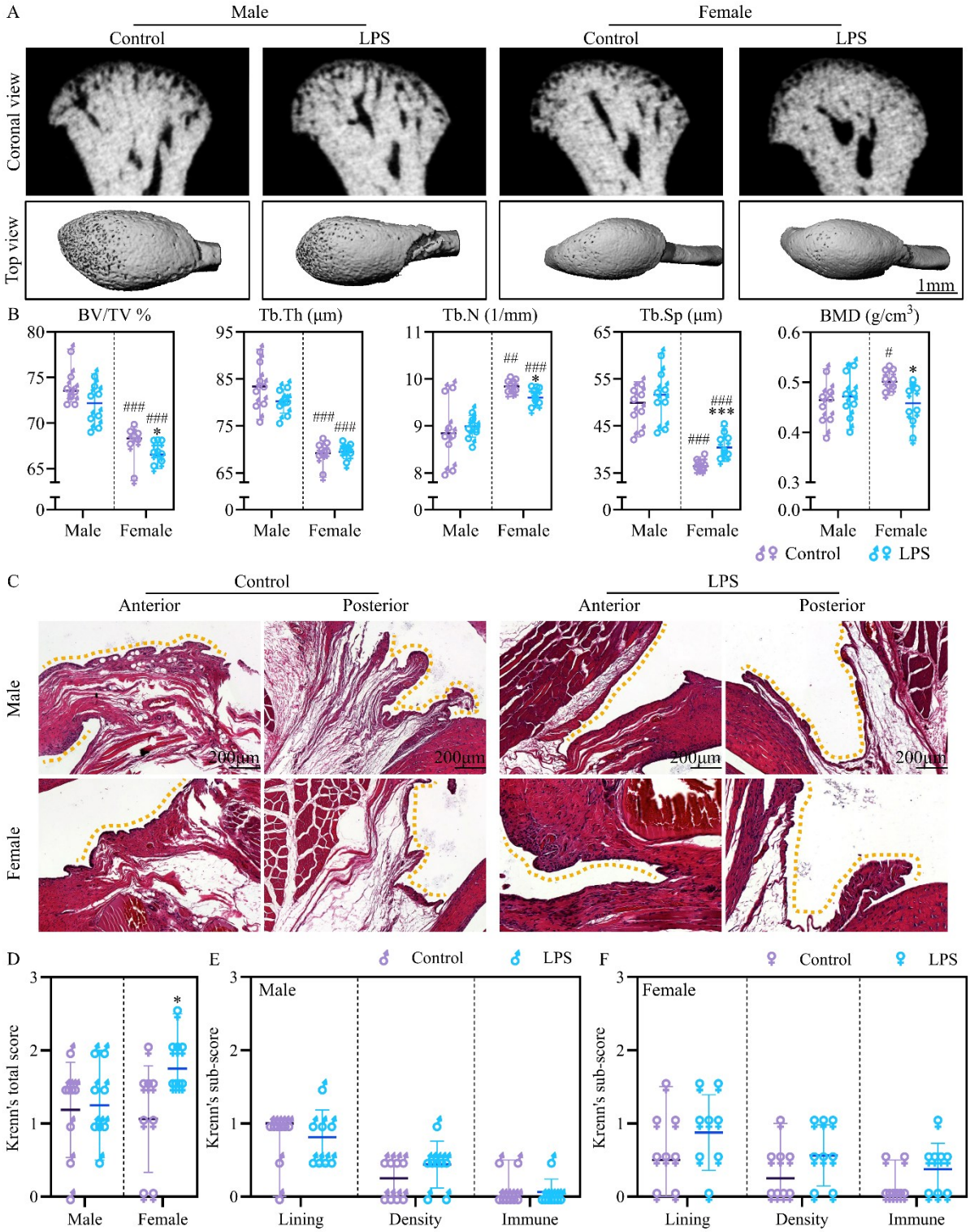

Figure 3. Assessment of subchondral bone structure and synovial membrane inflammation in TMJ. (A) Representative μCT images of TMJ condyles in coronal and top views. (B) Quantitative analysis of bone parameters. (C) Histological analysis of anterior and posterior TMJ synovial membrane using H&E staining; yellow dotted lines indicate the synovial lining layer. (D) Krenn's synovitis score used to assess overall synovial inflammation. Subcategory of Krenn's scores for (E) male and (F) female rats. N = 8 joints per group. Data are presented as median with 95% CI. * $P < 0.05$ compared to control group within same sex. $^{\#}$ $P < 0.05$, $^{\#\#}$ $P < 0.01$, $^{\#\#\#}$ $P < 0.001$ compared to the males within the same treatment group.

3.3. Spatial and sex-specific expression of leptin receptor and iNOS in TMJ cartilage

IF staining was performed to detect iNOS, a marker for oxidative stress, and Leptin receptor (LEP-R) expression in condylar cartilage (Figure 4A). The percentage of iNOS$^+$, LEP-R$^+$, and Double$^+$ cells in both top and hypertrophic layers of cartilage were quantified. In healthy controls, females showed a significantly higher percentage of iNOS$^+$ cells (32.74%, 95%CI: 19.37 – 44.15%, P = 0.038) and moderately more LEP-R$^+$ cells (39.21%, 95%CI: 24.04 – 64.19%) in the top layer compared to males (iNOS$^+$ cells: 5.20%, 95%CI: -0.33 – 22.60%; LEP-R$^+$ cells: 11.65%, 95%CI: 0.50 – 45.23%). As a result, 10.95% (95%CI: 3.85 – 21.56%) double$^+$ cells was found in top-layer cartilage in females, versus only 2.10% in males. LPS exposure further increase the population of LEP-R$^+$ (45.04%, 95%CI: 22.71 – 53.64) and Double$^+$ (15.98%, 95%CI: 5.59 – 31.31%) cells in female top-layer cartilage, however, having less impact in males (Figure 4B).

In the hypertrophic layer, both sexes showed higher baseline levels of iNOS$^+$ and LEP-R$^+$ cells compared to top layer. LPS increased the LEP-R$^+$ in males but unexpectedly reduced the double-positive cell population. In contrast, LPS had minimal effect on the phenotype of hypertrophic chondrocytes of female rats (Figure 4B).

Higher percentage of iNOS$^+$, LEP-R$^+$ and Double$^+$ cells in top layer moderately correlated with poorer bone parameters ($P < 0.05$) (Figure 4C). Interestingly, higher percentage of LEP-R$^+$ in hypertrophic layer positively correlates with Saf-O$^+$ stained area ($r = 0.484$, $N = 32$, $P = 0.005$), indicating a dual role of leptin signalling in cartilage homeostasis, depending on its spatial distribution.

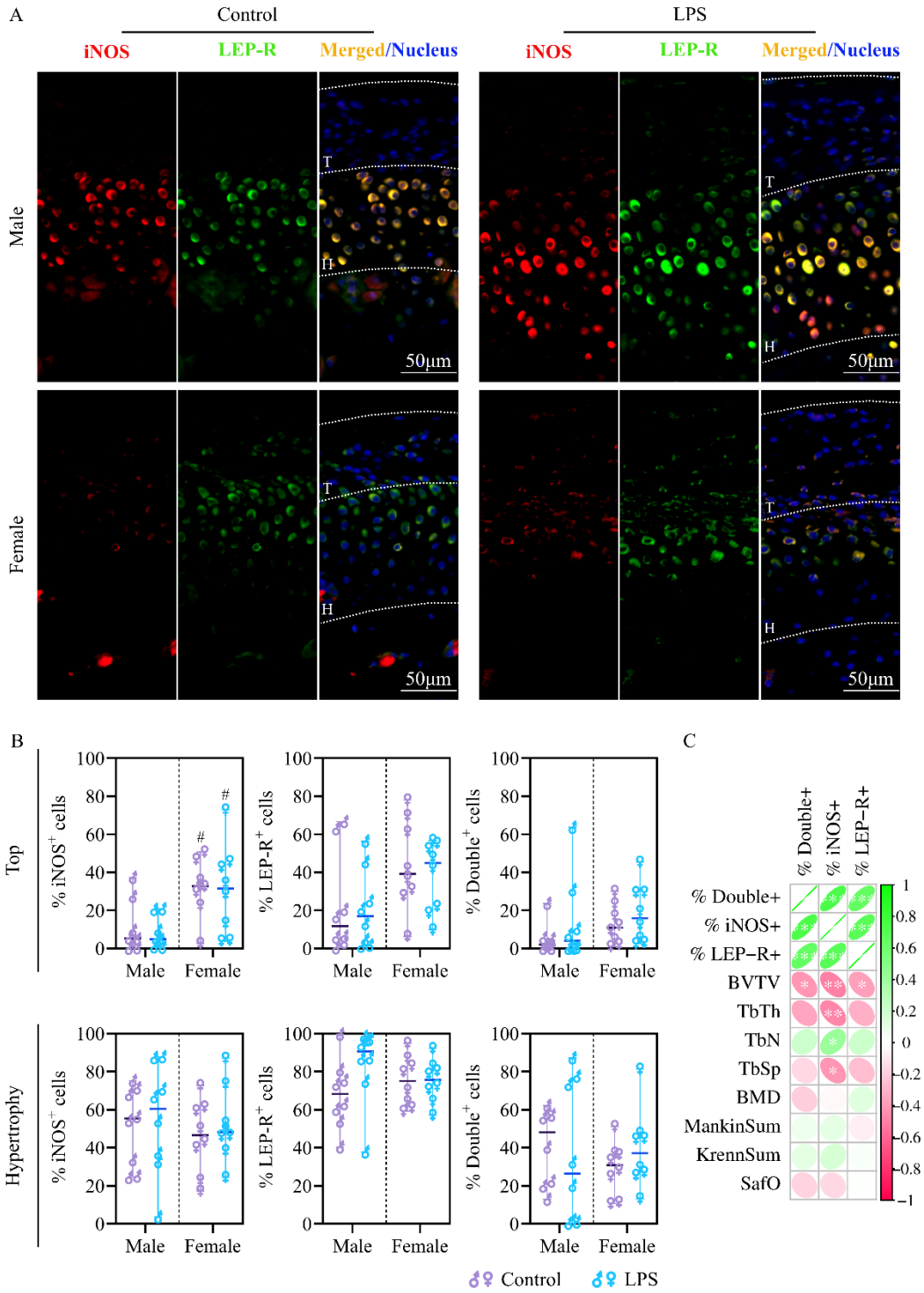

232

233 Figure 4. Leptin receptor and iNOS expression profile in TMJ cartilage and its association with
234 joint pathophysiology. (A) Representative IF images showing iNOS^{+} (red), LEP-R^{+} (Green),
235 Double^{+} (yellow) cells in top layer (T) and hypertrophic layer (H) of TMJ condylar cartilage.
236 (B) Quantitative analysis of iNOS^{+}, LEP-R^{+} and double+ cells. N = 8 joints per group. Data are
237 presented as median with 95% CI. $^{\#}$ $P < 0.05$, compared to the males within the same treatment
238 group. (C) Heatmap showing Spearman correlation between the percentage of iNOS^{+}, LEP-R^{+}
239 and double^{+} cells in the top layer with bone parameters, histopathological scores and % Saf-O^{+}
240 area. * $P < 0.05$, ** $P < 0.01$ for spearman's correlation coefficient.

Discussion

This study demonstrated that chronic exposure to LPS induced pathological changes in adipose and leptin in female rats. These systemic metabolic changes were associated with the development of TMJ OA in female, as evidenced by significant cartilage matrix loss, subchondral bone resorption and synovial inflammation. In contrast, male rats exhibited subtle surface irregularities and ECM fiber derangement. These findings highlighted a distinct sexual dimorphism in response to systemic LPS, both at metabolic and local joint levels. The potential contributing role of leptin-mediated pathway in female's susceptibility to TMJ OA was explored.

We showed in this study that chronic systemic delivery of LPS resulted in metabolic endotoxemia characterized by an increase of blood LPS concentration and abnormalities in adipose tissue. These observations are consistent with earlier findings (Cani et al. 2007). It's noteworthy that we used considerably lower dose of LPS than previous reports (Cani et al. 2007; Uchiumi et al. 2004), yet still sufficient to promote metabolic dysfunction. This discrepancy may be related to the differences in structural and biological properties of LPS, as different types of LPS can elicit distinct host metabolic activities (Anhê et al. 2021).

Sex difference in adipose storage and metabolism has been extensively discussed (Enzi et al. 1986; Mauvais-Jarvis 2015). Leptin is secreted from WAT in direct proportion to fat content, and it has better correlation with adiposity in female due to estrogen (Clegg et al. 2006). This sex difference is successfully recapitulated in our study. In female rats, LPS led to hypertrophic changes in adipocytes from both subcutaneous and visceral fat depots, accompanied by an increase in circulating leptin concentration, while this relationship was not observed in males, aligning with human observations (Kennedy et al. 1997).

Beyond its metabolic role, leptin has been implicated in OA through interactions with leptin receptors (Ait Eldjoudi et al. 2022). Leptin receptors are expressed in various peripheral tissues including bone and cartilage, where they were found to mediate inflammatory response through downstream iNOS signalling (Otero et al. 2005; Otero et al. 2003), as well as GAG synthesis (Figenschau et al. 2001) in chondrocytes. In our study, we observed the complex dual role of leptin receptor in relation to their spatial distribution. In healthy animals, LEP-R expressing chondrocytes were predominately located in the hypertrophic cartilage layer, where their presence was positively correlated to GAG deposition. LPS exposure did not alter LEP-R expression in hypertrophic chondrocytes but increased the population of LEP-R^{+} and LEP-R/iNOS double positive cells in the top cartilage layer of female rats. Together, these findings suggest a dual role for leptin signalling in TMJ cartilage, potentially catabolic in superficial fibrous chondrocytes and anabolic in deeper hypertrophic chondrocytes. Further investigation is needed to understand the complexity of leptin signaling in TMJ cartilage pathophysiology.

However, several limitations should be acknowledged in this proof-of-concept study. Firstly, the effect size of LPS was relatively low. Given the current sample size, we are unable to achieve 80% study power, making some results less conclusive. Secondly, although our data support an association between leptin signalling and joint pathology, *in vitro* studies using leptin agonist, antagonist or genetic modification models would be needed to understand the detailed mechanism of action. Lastly, anatomical and biomechanical differences between rat and human

TMJs may limit the translational relevance of our findings. Further validation in larger animal models or humanized *in vitro* system will be essential.

Conclusion

In conclusion, our findings demonstrated that chronic metabolic endotoxemia induces sex-specific TMJ OA development in rats via a leptin-associated inflammatory pathway. Female rats are particularly susceptible to circulating endotoxin, exhibiting more severe adipose tissue dysfunction, imbalanced leptin secretion and abnormal leptin receptor distribution in TMJ cartilage, leading to pronounced osteoarthritic changes. These results established a potential mechanistic link between systemic metabolic disorders and joint pathology, highlighting the differences between sexes. This study provides novel insights that may inform future drug development for TMJ OA.

Author Contributions

S.Zhang contributed to conception, design, data acquisition, analysis, and interpretation, drafted and critically revised the manuscript; S.Chen contributed to design, data acquisition, analysis, and interpretation, critically revised the manuscript; M.Fonti contributed to data acquisition, analysis, and critically revised the manuscript; D.Fercher contributed to design, data acquisition, and critically revised the manuscript. All authors gave final approval and agreed to be accountable for all aspects of the work.

Declaration of Conflicting interests

The authors declare no potential conflicts of interest with respect to research, authorship, and/or publication of this article.

Funding statement

This project has received funding from the European Union's Horizon Europe Research and innovation programme under grant agreement No 101095084. This work was supported by the Swiss State Secretariat for Education, Research and Innovation (SERI) under contract number 22.00462.

Reference

Ait Eldjoudi D, Cordero Barreal A, Gonzalez-Rodríguez M, Ruiz-Fernández C, Farrag Y, Farrag M, Lago F, Capuozzo M, Gonzalez-Gay MA, Mera Varela A et al. 2022. Leptin in osteoarthritis and rheumatoid arthritis: Player or bystander? International journal of molecular sciences. 23(5).

Altman DG, Bland JM. 1999. How to randomise. BMJ (Clinical research ed). 319(7211):703-704.

Alzahrani A, Yadav S, Gandhi V, Lurie AG, Tadinada A. 2020. Incidental findings of temporomandibular joint osteoarthritis and its variability based on age and sex. Imaging science in dentistry. 50(3):245-253.

Amar J, Burcelin R, Ruidavets JB, Cani PD, Fauvel J, Alessi MC, Chamontin B, Ferriéres J. 2008. Energy intake is associated with endotoxemia in apparently healthy men12. The American journal of clinical nutrition. 87(5):1219-1223.

Anhê FF, Barra NG, Cavallari JF, Henriksbo BD, Schertzer JD. 2021. Metabolic endotoxemia is dictated by the type of lipopolysaccharide. Cell Reports. 36(11):109691.

Asadikorayem M, Weber P, Zhang S, Surman F, Fercher D, Fonti M, Bevc K, Kauppinen S, Frondelius T, Finnilä MAJ et al. 2025. In-situ-forming zwitterionic hydrogel does not ameliorate osteoarthritis in vivo, despite protective effects ex vivo. Biomaterials Advances. 169:214151.

Bagchi DP, MacDougald OA. 2019. Identification and dissection of diverse mouse adipose depots. 1940-087X.

Cani PD, Amar J, Iglesias MA, Poggi M, Knauf C, Bastelica D, Neyrinck AM, Fava F, Tuohy KM, Chabo C et al. 2007. Metabolic endotoxemia initiates obesity and insulin resistance. Diabetes. 56(7):1761-1772.

Clegg DJ, Brown LM, Woods SC, Benoit SC. 2006. Gonadal hormones determine sensitivity to central leptin and insulin. Diabetes. 55(4):978-987.

Collins KH, Paul HA, Reimer RA, Seerattan RA, Hart DA, Herzog W. 2015. Relationship between inflammation, the gut microbiota, and metabolic osteoarthritis development: Studies in a rat model. Osteoarthritis and cartilage. 23(11):1989-1998.

Du J, Jiang Q, Mei L, Yang R, Wen J, Lin S, Li H. 2020. Effect of high fat diet and excessive compressive mechanical force on pathologic changes of temporomandibular joint. Scientific Reports. 10(1):17457.

Enzi G, Gasparo M, Biondetti PR, Fiore D, Semisa M, Zurlo F. 1986. Subcutaneous and visceral fat distribution according to sex, age, and overweight, evaluated by computed tomography. The American journal of clinical nutrition. 44(6):739-746.

Figenschau Y, Knutsen G, Shahazeydi S, Johansen O, Sveinbjörnsson B. 2001. Human articular chondrocytes express functional leptin receptors. Biochemical and Biophysical Research Communications. 287(1):190-197.

Kennedy A, Gettys TW, Watson P, Wallace P, Ganaway E, Pan Q, Garvey WT. 1997. The metabolic significance of leptin in humans: Gender-based differences in relationship to adiposity, insulin sensitivity, and energy expenditure*. The Journal of Clinical Endocrinology & Metabolism. 82(4):1293-1300.

Krenn V, Morawietz L, Burmester GR, Kinne RW, Mueller-Ladner U, Muller B, Haupl T. 2006. Synovitis score: Discrimination between chronic low-grade and high-grade synovitis. Histopathology. 49(4):358-364.

Lago R, Gómez R, Lago F, Gómez-Reino J, Gualillo O. 2008. Leptin beyond body weight regulation—current concepts concerning its role in immune function and inflammation. Cellular Immunology. 252(1):139-145.

Mankin HJ, Dorfman H, Lippiello L, Zarins A. 1971. Biochemical and metabolic abnormalities in articular cartilage from osteo-arthritic human hips. Ii. Correlation of morphology with biochemical and metabolic data. The Journal of bone and joint surgery American volume. 53(3):523-537.

Mauvais-Jarvis F. 2015. Sex differences in metabolic homeostasis, diabetes, and obesity. Biology of Sex Differences. 6(1):14.

Minervini G, Franco R, Marrapodi MM, Almeida LE, Ronsivalle V, Cicciù M. 2023. Prevalence of temporomandibular disorders (tmd) in obesity patients: A systematic review and meta-analysis. Journal of Oral Rehabilitation. 50(12):1544-1553.

Otero M, Lago R, Lago F, Reino JJ, Gualillo O. 2005. Signalling pathway involved in nitric oxide synthase type ii activation in chondrocytes: Synergistic effect of leptin with interleukin-1. Arthritis research & therapy. 7(3):R581-591.

Otero M, Reino JJG, Gualillo O. 2003. Synergistic induction of nitric oxide synthase type ii: In vitro effect of leptin and interferon-γ in human chondrocytes and atdc5 chondrogenic cells. Arthritis & Rheumatism. 48(2):404-409.

Pussinen PJ, Havulinna AS, Lehto M, Sundvall J, Salomaa V. 2011. Endotoxemia is associated with an increased risk of incident diabetes. Diabetes care. 34(2):392-397.

Rezakhaniha R, Agianniotis A, Schrauwen JTC, Griffa A, Sage D, Bouten CVC, van de Vosse FN, Unser M, Stergiopulos N. 2012. Experimental investigation of collagen waviness and orientation in the arterial adventitia using confocal laser scanning microscopy. Biomechanics and Modeling in Mechanobiology. 11(3):461-473.

Teichtahl AJ, Wluka AE, Proietto J, Cicuttini FM. 2005. Obesity and the female sex, risk factors for knee osteoarthritis that may be attributable to systemic or local leptin biosynthesis and its cellular effects. Medical Hypotheses. 65(2):312-315.

Trøseid M, Nestvold TK, Rudi K, Thoresen H, Nielsen EW, Lappegård KT. 2013. Plasma lipopolysaccharide is closely associated with glycemic control and abdominal obesity: Evidence from bariatric surgery. Diabetes care. 36(11):3627-3632.

Uchiumi D, Kobayashi M, Tachikawa T, Hasegawa K. 2004. Subcutaneous and continuous administration of lipopolysaccharide increases serum levels of triglyceride and monocyte chemoattractant protein-1 in rats. Journal of periodontal research. 39(2):120-128.

Wang XD, Zhang JN, Gan YH, Zhou YH. 2015. Current understanding of pathogenesis and treatment of tmj osteoarthritis. Journal of dental research. 94(5):666-673.

Weber P, Bevc K, Fercher D, Kauppinen S, Zhang S, Asadikorayem M, Marin LB, Zhang T, Frondelius T, Salzmann G et al. 2024. The collagenase-induced osteoarthritis (cioa) model: Where mechanical damage meets inflammation. Osteoarthritis and Cartilage Open. 6(4):100539.

Yadav S, Yang Y, Dutra EH, Robinson JL, Wadhwa S. 2018. Temporomandibular joint disorders in older adults. Journal of the American Geriatrics Society. 66(6):1213-1217.

Zhang S, Teo KYW, Chuah SJ, Lai RC, Lim SK, Toh WS. 2019. Msc exosomes alleviate temporomandibular joint osteoarthritis by attenuating inflammation and restoring matrix homeostasis. Biomaterials. 200:35-47.